International Journal of Engineering Technology and Management Sciences
Website: ijetms.in Issue: 2 Volume No.9 March - April – 2025
DOI:10.46647/ijetms.2025.v09i02.055 ISSN: 2581-4621

TiO_2 nano material synthesis, characterisation, and application in dye-sensitized solar cells with natural dye

Rishi Raj Prajapati[1], Deep Prakash Singh[1], Abhay Chauhan[1], Hemant Kumar Singh[1], Navin Chaurasiya[1], Sandip Kumar Singh[1] Kumkum Kumari[2] Aparna Singh Gaur[3]
[1]Department of Mechanical Engineering, V.B.S. Purvanchal University, Jaunpur, Uttar Pradesh, India
[2]Department of Chemistry, Pt. D. D. U. Government Degree College, Saidpur, Ghazipur, Uttar Pradesh, India.
[3]Department of Mechanical Engineering, Savitri Bai Phule Government Polytechnic, Azamgarh, Uttar Pradesh, India

Abstract
This work presents the synthesis of TiO_2 nanomaterials by the sol-gel method and explores its potential application in photovoltaic applications. X-ray diffraction (XRD), scanning electron microscopy (SEM), energy-dispersive X-ray spectroscopy (EDS), Fourier transform infrared (FTIR), and UV-Vis spectroscopy were among the methods used to characterise the synthesised TiO_2 nanomaterial. The crystalline phase with a minimum crystallite size of 23 nm is confirmed by XRD. While EDS verified the produced sample's elemental composition, SEM focused on the surface morphology and showed flower-like structures. The intended bond forms and the bandgap estimation were identified by FTIR and UV-Vis spectroscopy. Further, analysis of fabricated Dye-Sensitized Solar Cells (DSSCs) made up of natural dyes from spinach and beetroot and different sized TiO_2 nanoparticles, was performed using current-voltage (I-V) curves. According to the results, the power conversion efficiency is calculated to be 0.49% at an open circuit voltage of 338 mV, a short circuit current of 4.30 mA, and a fill factor of 0.483.

Introduction
Energy requirements have created widespread challenges of shortage of non-polluting and non-renewable energy resources worldwide. Among the various renewable energies, solar energy is the best and it is widely available throughout the year [1]. Developing clean alternatives to current power generation is imperative to protect the global environment. Photovoltaic devices generate electricity directly from sunlight without any emissions that can contribute to global warming.
Photovoltaic systems are classified based on their components: silicon, semiconductor thin films, organic, polymer, hybrid, and dye or QD sensitized. A dye-sensitized solar cell (DSSC) comprises mesoporous TiO_2 thick film, dye, redox electrolyte, and a counter electrode. Each component plays a role in electron transport and diffusion [2]. TiO_2 acts as a scaffold for the adsorbed dye molecules and photo generates electrons generated by light absorption and dye regeneration. Many efforts have been made to improve the TiO2 transport properties to enhance solar energy conversion in DSSCs. The morphology, particles, and pore size of TiO2 play an important role in the photoelectron diffusion and conversion efficiency of DSSCs [3]. In solar cells, the photon is converted into an electron and the conversion efficiency must be high. Among the different generations of solar cells, Dye-Sensitized Solar Cells (DSSC) is a third-generation solar cell having high performance and working in low light visible conditions compared to other generation solar cells [4]. TiO_2 nanomaterial with different morphologies spherical, tubes, wire, rhombic and squares have been synthesized by various methodologies, differences in morphology promote change in the crystallize size, band-gap energy, and surface area [5]. Materials properties can be modulated by synthesis conditions to decrease the material size, produce different shapes, or increase the surface

International Journal of Engineering Technology and Management Sciences
Website: ijetms.in Issue: 2 Volume No.9 March - April – 2025
DOI:10.46647/ijetms.2025.v09i02.055 ISSN: 2581-4621

to volume ration [6]. Since its commercial production TiO_2 has been subjecting of extensive research work to improve its properties, many methods are being employed in the synthesis of nano-crystalline TiO_2 with pure phase and specific shape as sol–gel, micelle and inverse micelle, sol, direct oxidation, chemical, microwave-assisted, and hydrothermal and solvothermal method. Hydrothermal and solvothermal methods present the advantage of simple operation conditions and the ability to produce TiO_2 nanomaterial with different shapes, high surface area, and controlled porosity.[8]
This study examines how variations in TiO_2 nanoparticle film particle size affect the total light conversion efficiency of the DSSC photo-anode. By adjusting the H_2O /Ti mole ratio, the diameter of the TiO_2 nanoparticle was modified through the use of the sol-gel method. Additionally, the produced TiO_2 powders' I-V curves were examined and compared in the presence of light.

2. Experimental Details

2.1 Chemicals Used

The chemicals utilized such as Titanium tetra iso-propoxide (TTIP; Sigma Aldrich, analytical grade), Nitric Acid (HNO_3), absolute Ethanol, and deionized water, were used to form TiO_2.

2.2 Synthesis Method

The synthesis of titanium dioxide (TiO_2) using the sol-gel method with titanium tetra iso-propoxide (TTIP) involves hydrolysis and condensation processes to produce TiO_2 nanoparticles or thin films. The procedure follows: 10 ml of TTIP was gradually added to 30 ml of ethanol with continuous stirring for 30 minutes. Then, a mixture of 3 ml of HNO_3 and 150 ml of deionized water was added dropwise over 2 hours along with stirring. After 12 hours, TiO_2 precipitated at the bottom of the flask, was separated by filtration, and dried at 100°C. The light-yellow product was obtained, ground, and then calcined at 450°C for 2 hours to produce TiO_2 Nano powder. The synthesis process is illustrated in the flowchart shown in Figure 1.

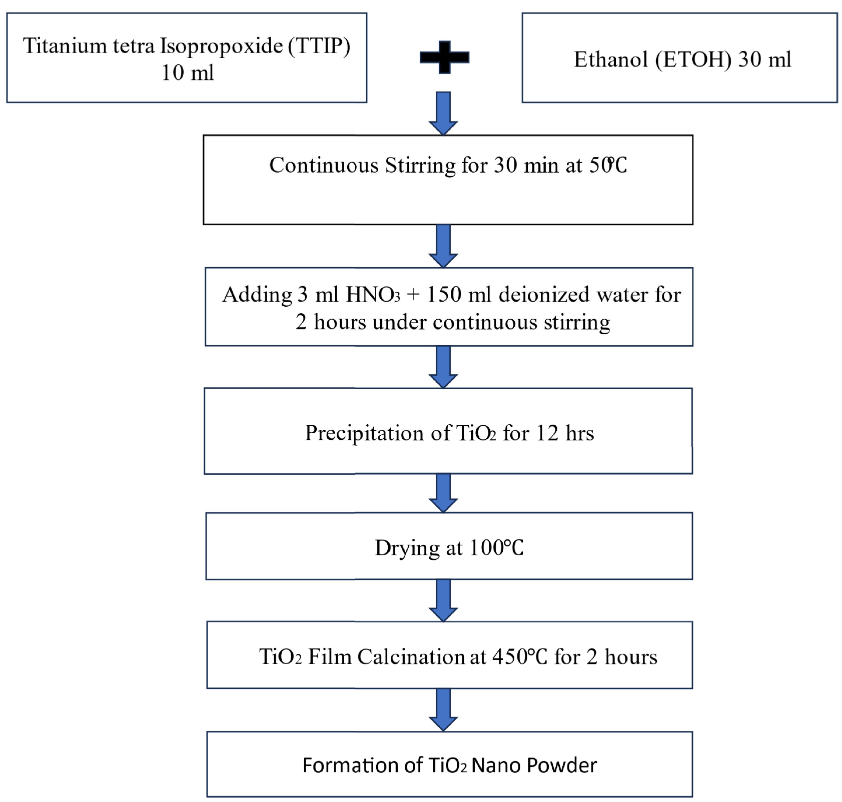

Figure 1: Flow Chart shows the Synthesis of Titanium dioxide (TiO_2) Nanomaterial

International Journal of Engineering Technology and Management Sciences
Website: ijetms.in Issue: 2 Volume No.9 March - April – 2025
DOI:10.46647/ijetms.2025.v09i02.055 ISSN: 2581-4621

2.3 Characterization details

Information about the crystallinity and phase formation was obtained using a powder X-ray diffractometer (XRD; D8 Advance Eco). The surface morphology of the synthesized material was analyzed using a Scanning Electron Microscope (SEM; JSM-6490LV, Jeol). The chemical bonds and their associated vibrational motions were examined using a Fourier Transform Infrared (FTIR) spectrophotometer (Nicolet 6700).

2.4 Fabrication of Dye-Sensitized Solar Cells

Figure 2 depicts the fabrication and assembly of Dye-Sensitized Solar Cells (DSSCs). Initially, 0.15 g of TiO_2 particles were mixed with 0.25 ml ethanol. This mixture was then thoroughly combined in a mortar to produce a TiO_2 slurry. Using the doctor blade method, TiO_2 pastes were applied to the conducting side of ITO glasses, forming the photoanodes with an effective active area of 1.44 cm^2. The coated glasses were dried on a hot plate for 15 minutes at 60 °C. A dye solution was prepared from the spinach (Chlorophyll) leaves and beetroot (Anthocyanin). Photoanode dipped in a dye solution for 10 min. and then washed in ethanol. For the counter electrode, Graphite was utilized as the conducting surface on the alternative ITO glass to serve as the counter electrode. Finally, the DSSCs were assembled, injecting the electrolyte between the photoanode and the counter electrode.

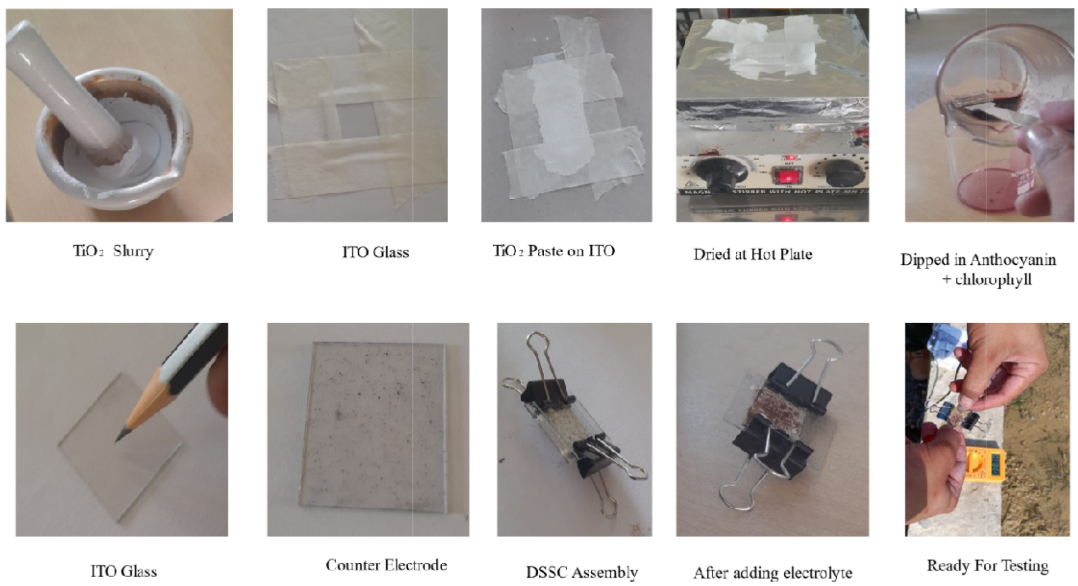

Figure 2: Dye Sensitized Solar Cell (DSSCs) Assembly

3. Results and Discussion

3.1 X-ray diffraction (XRD)

The crystalline characteristics of the substance are confirmed by the TiO_2 nanoparticles' fine powder XRD pattern, which is depicted in Figure 3. The characteristic peaks of TiO_2, which are directly tied to the JCPDS file no. 01-073-1764. The diffraction peaks (101), (202), (211), (004), (200), (211), (311), (221) and (310) respectively. The XRD peak broadening was used to determine the size of the crystal domains, and it was calculated from the full widths at half maximum height using the Debye- Scherer equation-

$$D = \frac{K\lambda}{\beta \cos\theta}$$

where,

λ is the incident beam's X-Ray wavelength, θ is the Bragg angle, and K is a constant roughly equal to 0.9, related to the domain shape. The average and smallest crystalline size of the synthesized TiO_2 nanoparticles was estimated to be 36 nm and 23 nm.

International Journal of Engineering Technology and Management Sciences
Website: ijetms.in Issue: 2 Volume No.9 March - April – 2025
DOI:10.46647/ijetms.2025.v09i02.055 ISSN: 2581-4621

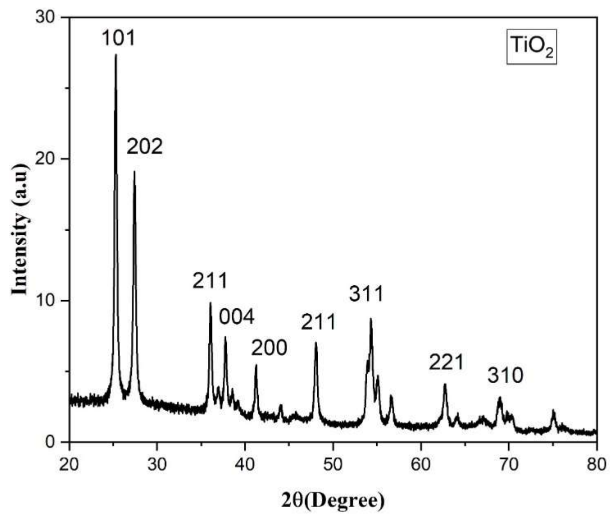

Figure 3: X-ray diffraction pattern of TiO2 nanoparticles

3.2. Scanning electron microscope (SEM) and energy dispersive X-ray spectroscopy (EDS)

Figure 4 (a, b) displays the surface morphology of TiO_2 nanoparticles at various magnifications (4.28, 18.0, 72.0 and 143 kx) and sizes (20 µm, 2 µm, 1 µm and 500 nm). The surface morphology amplifies the surface-to-volume ratio by clearly demonstrating that the TiO_2 nanoparticles were formed as flower like structures and have porosity also. This improved surface-to-volume ratio offers more surface area for capture the gases, making it beneficial for sensing applications. Additionally, the EDS spectrum depicted in Figure 4 (c) was employed to look into the purity and chemical make-up of TiO_2 nanoparticles. The presence of Ti (17.4 %) and O (58.9 %) components is verified by this spectrum and map data shows the density of the Ti and O at specific region which is also shown in the figure.

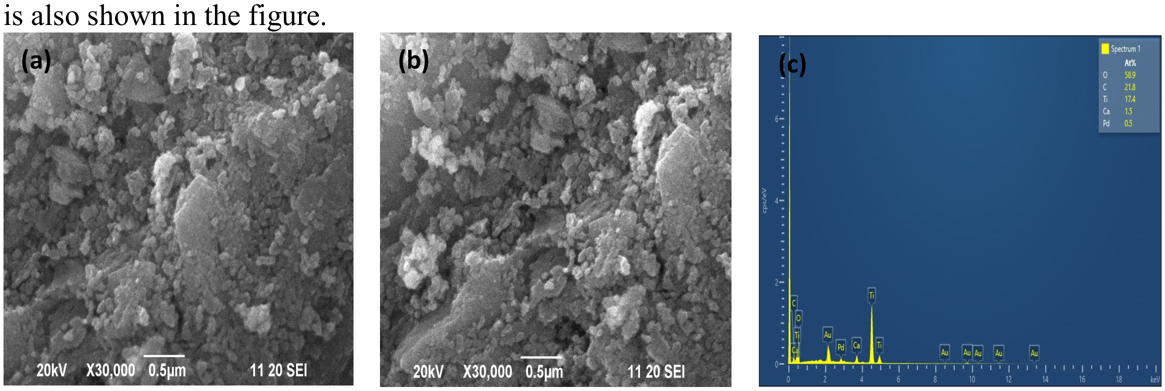

Figure 4. (a, b) SEM of TiO_2 at different magnification. (c) Elemental composition of TiO_2 using EDS.

3.3 Fourier-transform infrared spectroscopy (FTIR)

The FTIR method can be used to examine the structural specifics of the synthesized sample as well as generate an infrared spectrum of an object's absorption or emission. High-resolution spectral data are concurrently collected throughout a broad spectral range using an FTIR spectrometer. Figure 5 contrasts the transmittances for TiO_2 nanoparticles produced by the chemical procedure with the FTIR spectra obtained in the solid phase using the KBr pellet approach. The band at around 1413 cm^{-1} indicates the presence of O-H bending, medium appearance and carboxylic acid compound class. The band at about 974 cm^{-1} indicates the presence of C=C bending, strong appearance, trans distributed and the alkene compound class. The C-H bending strong appearance, and 1,2,4- tri-

International Journal of Engineering Technology and Management Sciences
Website: ijetms.in Issue: 2 Volume No.9 March - April – 2025
DOI:10.46647/ijetms.2025.v09i02.055 ISSN: 2581-4621

substituted compound class of the nanoparticles reach their apex at about 878 cm-1and the band about 520 cm^{-1} indicates the presence of C-Br stretching and strong appearance.

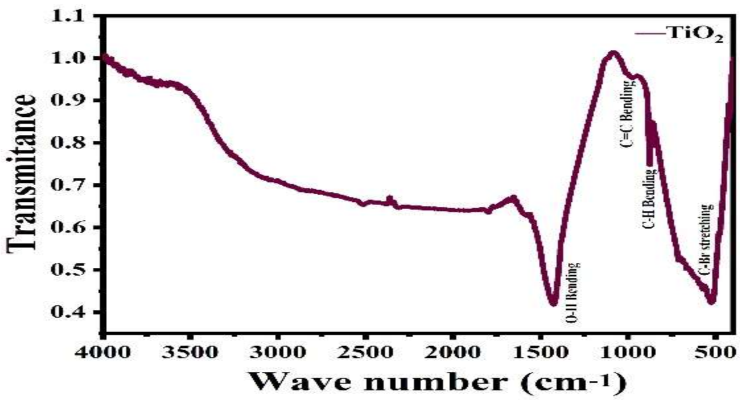

Figure 5. Fourier transform infrared spectrum of TiO_2 nanoparticles

3.4 Characterstics of Dye-Sensitized Solar Cells

The efficiency of a solar cell is intricately influenced by the spectral composition and intensity of the incident solar radiation, as well as the operational temperature of the solar cell. The determination of this efficiency necessitates a meticulously controlled and stable environment. The air mass ratio is 1.5 for standard efficiency assessments, and the temperature is standardized to 25°C.

A resistance box was interfaced with the solar cell to modulate the load resistance methodically. As shown in Table 1 corresponding to each resistance setting, the voltage (V) across the load and the current (I) traversing through it were meticulously quantified. The resultant power output (P) was deduced as the mathematical product of voltage and current (P=V×I), enabling the determination of the maximum power output (Pmax) across varying resistance conditions. At null resistance, the current attained its zenith, termed the short-circuit current (Isc), while at infinite resistance (open circuit), the voltage reached its apex, known as the open-circuit voltage (Voc). This investigation elucidates the relationship between load resistance and the solar cell's operational parameters, emphasizing the critical points where power output peaks.

Table 1. Variation of voltage and Current with varying resistance

Sr. No.	Resistance (Ω)	Voltage(V)	Current(mA)	Power(mW)
1	-	0	4.3	-
2	5	0.136	4.3	0.585
3	10	0.148	3.8	0.562
4	20	0.150	3.5	0.525
5	40	0.190	3.1	0.589
6	50	0.209	3	0.627
7	100	0.223	3	0.669
8	200	0.242	2.9	0.702
9	500	0.254	2.4	0.610
10	700	0.271	2.3	0.623
11	1000	0.284	1.7	0.483
12	2000	0.304	1.2	0.365
13	5000	0.316	0.6	0.190
14	10000	0.323	0.2	0.065
15	-	0.338	0	-

International Journal of Engineering Technology and Management Sciences
Website: ijetms.in Issue: 2 Volume No.9 March - April – 2025
DOI:10.46647/ijetms.2025.v09i02.055 ISSN: 2581-4621

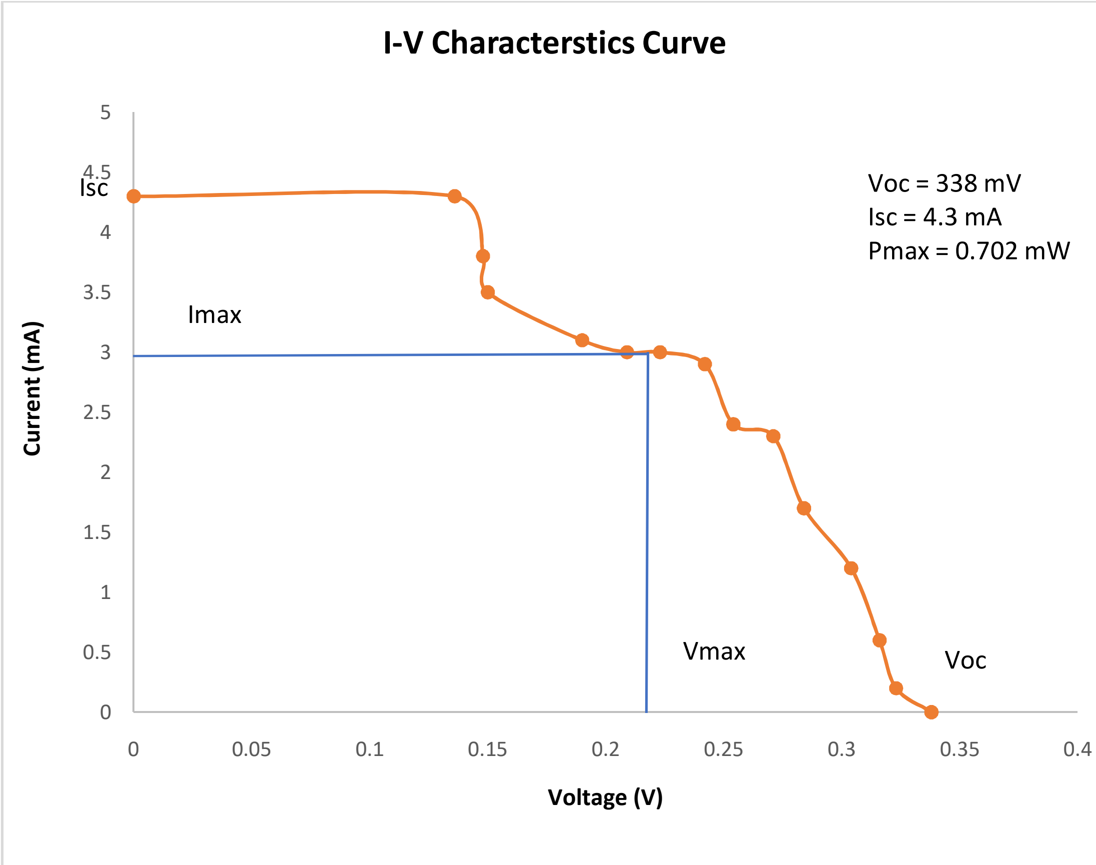

Figure 6: Characteristics of (I-V) Dye-sensitized solar cell

Figure 6 depicts voltage versus current plot, and the maximum power output was determined by calculating the area under the characteristic curve along the voltage axis. By considering the maximum current Im (milliamperes) and the maximum voltage Vm (volts), the maximum power Pm (milliwatts) was obtained. The morphology of the curve indicates proficient photo generation of charge carriers; however, it reveals inefficiencies arising from electron transport losses and recombination phenomena. Optimizations in the fill factor and photo voltage parameters would facilitate a substantial enhancement in the aggregate efficiency.

The photoelectric conversion efficiency of DSSC was inspected under the simulated sunlight source (AM1.5). With the current-voltage (I–V) curve taken as the foundation, the fill factor (FF) was defined as follows:

$$FF = \frac{Imax \times Vmax}{Isc \times Voc} \qquad (1)$$

where Imax and Vmax denote the maximum output value of current and voltage respectively, here from Table 1. Imax = 2.9 mA and Vmax = 0.242 V .The short-circuit current and open-circuit voltage, Isc = 4.3 mA and Vsc = 0.338 V respectively. The fill factor as obtained from equation 1 is FF = 0.483. The power conversion efficiency was defined as follows:

$$\eta = \frac{Isc \times Voc \times FF}{Pin} \times 100 \qquad (2)$$

The input power is 100 mW/cm². For an area of 1.44 cm², this results in an input power of 144 mW/cm². Using equation 2, the power conversion efficiency, η, is determined to be 0.49%.

The operational mechanism of a thin-film photovoltaic cell is based on the excitation of free electrons, which absorb energy from incident photons striking the film's surface, thereby undergoing electron transitions. In the context of TiO_2 synthesis and the fabrication of Dye-Sensitized Solar Cells (DSSCs) using natural dyes, efficiency improvements could be achieved by

International Journal of Engineering Technology and Management Sciences
Website: ijetms.in Issue: 2 Volume No.9 March - April – 2025
DOI:10.46647/ijetms.2025.v09i02.055 ISSN: 2581-4621

exploring alternative synthesis methodologies, employing different nanostructural configurations, utilizing synthetic dyes, or incorporating doping strategies, as evidenced by advancements in comparable research.

Conclusion

In this study, titanium dioxide was synthesized with a crystalline structure and an average size of 36 nm. It demonstrates a morphology of a flower-like porous structure led to an enhanced surface area. The TiO_2 nanoparticles were successfully applied as photo-anodes in the fabrication of dye-sensitized solar cells (DSSCs). The I-V characteristic curve of the DSSCs, assembled with natural dyes, exhibits peak power output at 200 Ω resistance, where the potential difference is quantified as 0.242 V, the electric current as 2.9 mA, and the resultant power dissipation as 0.702 mW. Further, the photoelectric conversion efficiency was estimated as 0.49%, considering an open circuit voltage of 338 mV, a short circuit current of 4.3 mA, and a fill factor of 0.483. Therefore, the TiO_2-based DSSCs seem to have a possible potential for harnessing renewable energy resources in a sustainable manner.

References

1. T. Raguram, K.S. Rajni, Influence of boron doping on the structural, spectral, optical and morphological properties of TiO_2 nanoparticles synthesized by sol–gel technique for DSSC applications, 33,5, 2110-2115 (2020).
2. C.-R. Lee, H.-S. Kim & N.- G. Park, Dependence of porosity, charge recombination kinetics and photovoltaic performance on annealing condition of TiO_2 films, 4,59-64 (2011).
3. N. Chaurasiya, U. Kumar, S. Sikarwar, B.C. Yadav, P. K. Yadawa, Synthesis of TiO_2 nanorods using wet chemical method and their photovoltaic and humidity sensing applications, Sensors International, 2, 100095 (2021).
4. D. Zhao, T. Peng, L. Lu, C. Ping, P. Jiang, Z. Bian, Effect of Annealing Temperature on the Photoelectrochemical Properties of Dye-Sensitized Solar Cells Made with Mesoporous TiO_2 Nanoparticles, 112,22,8486-8494 (2008).
5. S. Aksoy, O. Polat, K. Gorgun, Y. Caglar, M. Caglar, Li doped ZnO based DSSC: Characterization and preparation of nanopowders and electrical performance of its DSSC, 121,114127 (2020).
6. H. Zhang, H. Zhang, P. Zhu, F. Huang, Morphological Effect in Photocatalytic Degradation of Direct Blue over Mesoporous TiO_2 catalysts, 2, 3282-3288 (2017).
7. A. P. Alivisatos, Perspectives on the Physical Chemistry of Semiconductor Nanocrystals, 100, 31, 13226-13239 (1996).
8. X. Li, W. Zheng, G. He, R. Zhao, D. Liu, Morphology Control of TiO_2 Nanoparticle in Microemulsion and Its Photocatalytic Property, 2, 2, 288-295 (2014)
9. Tsakalakos, L. (2010). Introduction to photovoltaic physics, applications, and technologies. In Nanotechnology for Photovoltaics (pp. 19-66). CRC Press.
10. Almosni, S., Delamarre, A., Jehl, Z., Suchet, D., Cojocaru, L., Giteau, M., ... & Guillemoles, J. F. (2018). Material challenges for solar cells in the twenty-first century: directions in emerging technologies. Science and Technology of advanced MaTerialS, 19(1), 336-369.
11. Luque, A., & Hegedus, S. (Eds.). (2011). Handbook of photovoltaic science and engineering. John Wiley & Sons.
12. Dunlap-Shohl, W. A., Zhou, Y., Padture, N. P., & Mitzi, D. B. (2018). Synthetic approaches for halide perovskite thin films. Chemical reviews, 119(5), 3193-3295.
13. Govindasamy, G., Murugasen, P., & Sagadevan, S. (2016). Investigations on the synthesis, optical and electrical properties of TiO 2 thin films by chemical bath deposition (CBD) method. Materials Research, 19, 413-419.
14. Arora, B., Murar, M., & Dhumale, V. (2015). Antimicrobial potential of TiO2 nanoparticles against MDR Pseudomonas aeruginosa. Journal of Experimental Nanoscience, 10(11), 819-827.

International Journal of Engineering Technology and Management Sciences
Website: ijetms.in Issue: 2 Volume No.9 March - April – 2025
DOI:10.46647/ijetms.2025.v09i02.055 ISSN: 2581-4621

15. Mo, S. D., & Ching, W. Y. (1995). Electronic and optical properties of three phases of titanium dioxide: Rutile, anatase, and brookite. Physical review B, 51(19), 13023.
16. Li, Y., Zhang, S., Yu, Q., & Yin, W. (2007). The effects of activated carbon supports on the structure and properties of TiO2 nanoparticles prepared by a sol–gel method. Applied Surface Science, 253(23), 9254-9258.
17. Moellmann, J., Ehrlich, S., Tonner, R., & Grimme, S. (2012). A DFT-D study of structural and energetic properties of TiO2 modifications. Journal of physics: condensed matter, 24(42), 424206.
18. Hoang, V. V., Zung, H., & Trong, N. B. (2007). Structural properties of amorphous TiO 2 nanoparticles. The European Physical Journal D, 44, 515-524.
19. Mahmoud, W. M., Rastogi, T., & Kümmerer, K. (2017). Application of titanium dioxide nanoparticles as a photocatalyst for the removal of micropollutants such as pharmaceuticals from water. Current Opinion in Green and Sustainable Chemistry, 6, 1-10.
20. Tasić, N., Stanojević, Z. M., Branković, Z., Lačnjevac, U., Ribić, V., Žunić, M., ... & Branković, G. (2016). Mesoporous films prepared from synthesized TiO2 nanoparticles and their application in dye-sensitized solar cells (DSSCs). Electrochimica Acta, 210, 606-614.
21. Kumar, V., Singh, A., Yadav, B. C., Singh, H. K., Singh, D. P., Singh, S. K., & Chaurasiya, N. (2023). Environment-sensitive and fast room temperature CO2 gas sensor based on ZnO, NiO and Ni-ZnO nanocomposite materials. Environmental Functional Materials, 2(2), 167-177.